The sweet key: to unlocking full dendritic cell potential

Li, R.J.E.

2020

document version
Publisher's PDF, also known as Version of record

frontiers in Cell and Developmental Biology

doi: 10.3389/fcell.2020.00556

CHAPTER 3

TARGETING OF THE LANGERHANS CELL C-TYPE LECTIN RECEPTOR LANGERIN USING BIFUNCTIONAL MANNOSYLATED ANTIGENS

R.J. Eveline Li and Tim P. Hogervorst,
Silvia Achilli
Sven C. Bruijns
Sander Spiekstra
Corinne Vivès
Michel Thépaut
Dmitri V Filippov
Gijs A. van der Marel
Sandra J. van Vliet
Franck Fieschi
Jeroen D.C. Codée and Yvette van Kooyk

ABSTRACT

Langerhans cells are antigen presenting cells that reside in the skin. They uniquely express high levels of the C-type lectin receptor (CLR) Langerin (CD207), which is an attractive target for antigen delivery in immunotherapeutic vaccination strategies against cancer. We here assess a library of 20 synthetic, well-defined mannoside clusters, built up from one, two, three of six mono-, di- or trimannosides, appended to an oligopeptide backbone, for binding with Langerin using Surface Plasmon Resonance and flow cytometric quantification. It is found that Langerin binding affinity increases with increasing number of mannosides. Hexavalent presentation of the mannosides resulted in binding affinities ranging from 3 to 12 μM. Trivalent presentation of the di- and trimannosides led to Langerin affinity in the same range. The model melanoma gp100 antigenic peptide was subsequently equipped with a hexavalent cluster of the di- and trimannosides as targeting moieties. Surprisingly, although the bifunctional conjugates were taken up in Langerhans cells in a Langerin dependent manner, limited antigen presentation to cytotoxic T cells was observed. These results indicate that targeting glycan moieties on immunotherapeutic vaccines should not only be validated for target binding, but also on the continued effects on biology, such as antigen presentation to both $CD8^+$ and $CD4^+$ T cells.

INTRODUCTION

Immunotherapeutic vaccination is an appealing approach to direct the immune response towards specific tumor cells. The human skin is an obvious vaccination site for anti-tumor therapies. Multiple antigen presenting cell (APC) populations are present in the different layers of the skin, where they are key players in the activation of the adaptive immune response. Langerhans cells (LCs) are professional APCs that reside in the dermis, representing 1-5% of the epidermal cells[1]. LCs have been determined large contributors to in vivo antigen cross-priming and play a key role in the induction of T_H1 and T_H17 responses by antigen-specific $CD4^+$ T cells[2]. Depletion of LCs highly affected therapeutic epicutaneous immunization against cancer cells, and reduced the protection by the immune system against tumor growth[3].

Langerhans cells specifically express the C-type Lectin receptor (CLR) Langerin (CD207)[4], which is a pattern recognition receptor (PRR), binding carbohydrate structures such as $Lewis^Y$ antigens and oligomannosides[5]. The Langerin receptor has been targeted for its endocytic and immunomodulatory properties. Liposome functionalization with heparin-derived monosaccharide analogues enhanced Langerin-mediated endocytosis[6]. By targeted delivery with antibody conjugates, enhanced antigen presentation to $CD8^+$ and $CD4^+$ T cells could be established[7]. Langerin targeting could also be established with fucosylated synthetic long peptide antigens, which resulted in enhanced antigen presentation by Langerhans cells and cross-presentation[8]. The exploitation of mannosides for targeting Langerin has been minimally explored due to the presence of many other mannose-binding CLRs, including DC-SIGN[9–11].

To identify the optimal oligomannoside structure for Langerin targeting, we have used a library of 20 mannose ligands, which we have previously assessed for DC-SIGN binding. The library is built up from clusters of mannosides, appended to a peptide backbone. Five (oligo)mannoside structures (Man; Manα1-2Man; Manα1-3Man; Manα1-6Man; and Manα1-3[Manα1-6]Man saccharides), each representing a substructure of the high affinity Man_9 oligosaccharide, were used to build the library. The library members systematically vary in saccharide structure (coded **A**-**E**) and number of copies on the peptide scaffold (n = 1, 2, 3, 6, Figure 1A, Sl.Figure 1)[12].

RESULTS AND DISCUSSION

To determine Langerin extracellular domain (ECD) binding affinity, we measured interactions with surface plasmon resonance (SPR) assays. On the cell surface, Langerin oligomerizes into a trimer for high affinity ligand engagement[13]. Therefore, in the SPR

assays we made use of a trimeric Langerin ECD attached on the surfaces by the N-termini of their neck domain, to mimic the natural presentation of the carbohydrate recognition domains at the cell membrane[5]. In the direct interaction mode, where the Langerin ECD was bound to the sensor chip surface facing the ligands in the solvent, the apparent K_d was calculated for the ligands. Hexavalent presentation of the saccharides corresponded to binding affinities in a 3-12 µM range, which is sufficient for Langerin targeting purposes (Figure 1B). The affinity of the Manα1-6Man glycan **D6**, was approximately four-fold lower than to the other hexavalent di-mannosides (12.3 µM for **D6**, versus 3.2 µM for **B6** and 3.9 µM for **C6**), suggesting that Langerin is able to differentiate between the dimannoside structures. This finding is consistent with crystallographic analysis where Manα1-2Man and Manα1-3Man were found binding to the monomeric Langerin CRD, revealing preferential binding of these disaccharides to Langerin[5]. Surprisingly, no significant affinity difference was observed between the trivalent and hexavalent presentation of the same Manα1-6Man glycan (from 9.8 to 12.3 µM). The same phenomenon was seen with the Manα1-3[Manα1-6]Man **E6** (from 6.5 to 4.23 µM), while the binding affinity of saccharides **A** and **B** improved by at least thirteen-fold from the trivalent to the hexavalent presentation. To quantify binding of the low affinity ligands, IC_{50} values were assessed with a competition assay using the same trimeric Langerin ECD. Langerin affinity decreased with lower numbers of mannoside copies. Of the monovalent saccharides, only **B1** had a binding affinity in the mM range, indicating that the affinity of the other mannosides for Langerin is too weak to be determined in this assay.

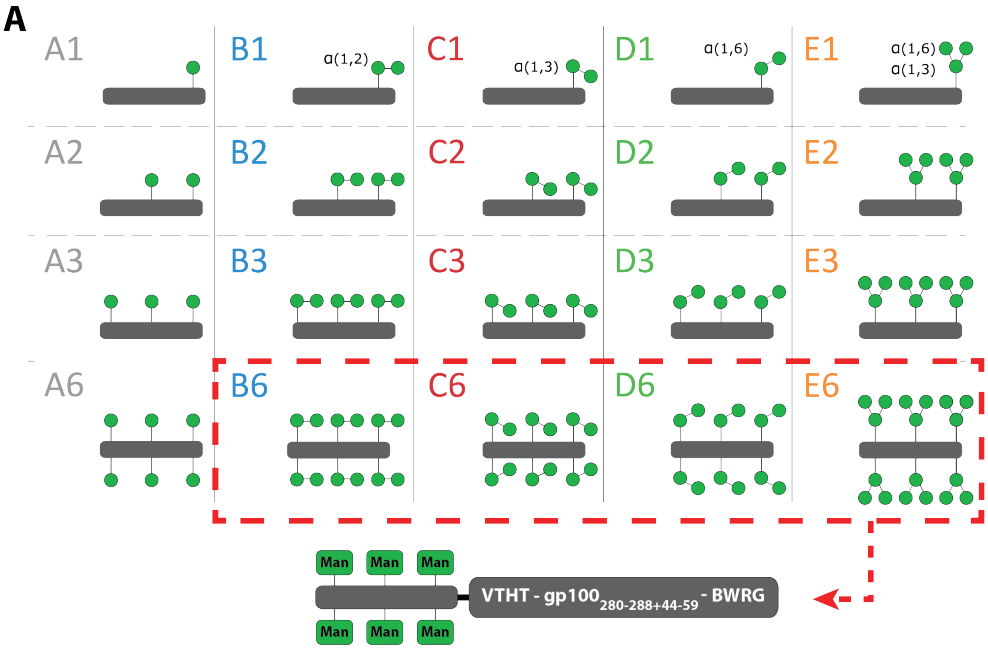

B

Ligand	IC_{50} (μM)	Kd_{app} (μM)
A1	N.D.	
A2	2424 ± 30	
A3		43
A6		3.4 ± 1.4
B1	4138 ± 773	
B2	181 ± 4	
B3		48
B6		3.2 ± 1.7
C1	N.D.	
C2	1415 ± 13	
C3	281 ± 14	
C6		3.9 ± 1.5
D1	N.D.	
D2		16
D3		9.8
D6		12.3 ± 0.7
E1	N.D.	
E2		278
E3		4.23
E6		6.5 ± 2.7

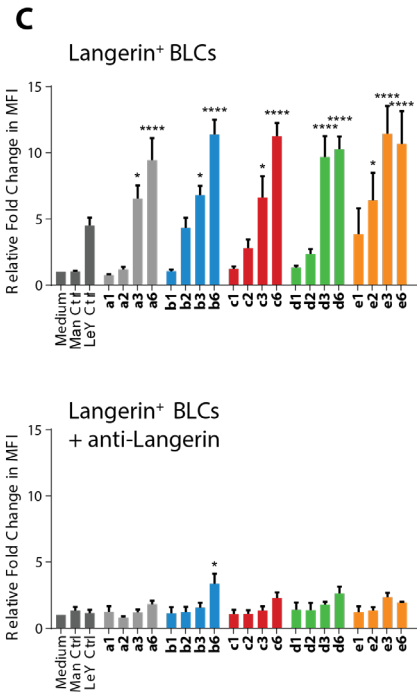

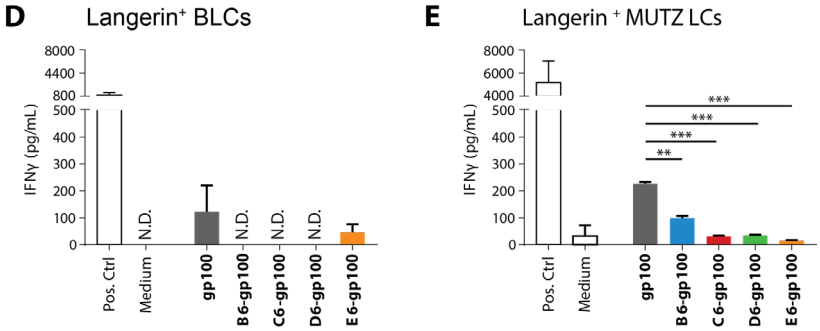

Figure 1 | The binding and antigen presentation profiles of the mannoside clusters. (A) A schematic overview of the 20 mannoside clusters. Only the hexavalent clusters are further conjugated to a gp100 antigen. (B) Surface plasmon resonance (SPR) analysis demonstrates increase of Langerin affinity with increased multivalency (n = 1 > 2 > 3 > 6). All hexavalent clusters bind within an approximate 10 μM range. (C) Binding of biotin-functionalized clusters to Langerin+ BLCs was measured by flow cytometry. Normalized to medium, the binding profiles mirror the SPR data, where higher multivalent presentation of the saccharides significantly increases the receptor binding compared to medium. The binding is inhibited by blocking with a Langerin-binding antibody. (D) Antigen presentation by the Langerin+ BLCs was measured by IFNγ release of activated T cells. Mannosylated antigens are not presented. Low levels of **E6-gp100** activated T cells could be measured, although at lower levels than for the **gp100** control. Data are representative of three independent experiments with $gp100_{280-288}$ as positive control, and is represented as average ± SD, N.D. = not determined (E) Antigen presentation by the Langerin+ MUTZ-3 LCs was measured by IFNγ release of activated T cells. Mannosylation of the gp100 antigen significantly reduced antigen presentation compared to the gp100 control. *p < 0.05, **p < 0.01, and ***p < 0.001

We continued to validate cluster binding on Langerin$^+$ cells, using a Langerin expressing human Epstein-Barr virus-transformed B-lymphoblastic cell line (BLCs) (Sl.Figure 2)[14]. The cells were pulsed with biotin-functionalized clusters (indicated with lowercase letter codes in Figure 1C) for 30 minutes at 4°C before staining with fluorescent-labelled streptavidin and flow cytometric quantification. The clusters presenting three or six copies of the Man, Manα1-2Man, and Manα1-3Man saccharides (**a3**, **a6**, **b3**, **b6**, **c3**, **c6**) showed significantly increased Langerin binding compared to the unstimulated control (Figure 1C), in line with the SPR assay. For the Manα1-6Man and trimannosides, the binding of the trivalent clusters (**d3** and **e3**) was very similar to the binding of the corresponding hexavalent constructs (**d6** and **e6**), as observed in SPR assays. Binding of the clusters could be blocked using a Langerin-specific antibody, confirming Langerin binding specificity of the mannosylated clusters. Taken together, the findings of the binding assays indicate that Langerin affinity depends on the nature of the oligomannosides and that it can be improved through multivalency. Overall, the hexavalent presentation of the mannoside provided ligands with high Langerin affinity, encouraging the application of these constructs for *in vivo* targeting of the Langerin receptor.

Previously it has been demonstrated that Lewis^Y-functionalized peptides can be used as vaccine modalities targeting Langerin for enhanced antigen presentation[15]. We therefore explored whether the appendage of the mannose clusters to a tumor-associated antigen could have a similar effect. We selected the melanoma-associated gp100 antigen as a well-known tumor-associated model antigen. As previously described, azidolysine functionalized $gp100_{280\text{-}288+44\text{-}59}$ antigens were synthesized using automated Fmoc-based solid phase peptide synthesis (SPPS) and conjugated to propargyl functionalized **B6**, **C6**, **D6**, **E6** clusters to generate bifunctional mannosylated antigens (Figure 1A)[12]. Four natural occurring amino acids $gp100_{276\text{-}279}$ were used as spacer between the two moieties.

Pathogen encounter in the skin causes the LCs to undergo genetic reprogramming. The cell focus shifts from endocytosis to efficient antigen processing and presentation, along with altered cytokine secretion for naïve T cell priming and cell migration towards the lymphoid organs[16,17]. To study the capacity of the bifunctional conjugates to induce antigen presentation, we quantified T cell activation. A $gp100_{280\text{-}288}$ peptide-specific CD8$^+$ T cell clone was used in this assay, which secretes IFNγ upon interaction with the APC-presented gp100 antigen. The BLCs were stimulated for 30 minutes with the conjugates, where after the compounds were washed away. After overnight stimulation with the T cells, the secreted IFNγ in the medium was measured through ELISA. The $gp100_{280\text{-}288}$ short peptide was used as positive control for antigen recognition by CD8$^+$ T cells in MHC-I molecules. Surprisingly, minimal T cell activation was measured upon stimulation with the mannosylated antigens, while the use of the **gp100** peptide as stand-alone antigen

was able to induce activation (Figure 1D).

To probe antigen presentation induction by the bifunctional conjugates in a different model, we employed *in vitro* generated human MUTZ-3 cell line-derived Langerhans cells. The MUTZ-3-derived LCs are an established model to study Langerin-pathogen interactions with e.g. HIV[18,19]. After 30 minutes stimulation with the mannosylated antigens, the MUTZ-3 cells were washed and co-cultured with the $gp100_{280-288}$-restricted T cell clone, after which T-cell activation was measured as described above. In this set-up we were able to measure T cell activation by the bifunctional conjugates (Figure 1E), however antigen presentation with all mannosylated conjugates was significantly lower than the unglycosylated **gp100** antigen, in line with the results obtained in the BLC-assay.

These results stand in contrast to previous reports that have demonstrated that Langerin-mediated internalization of $Lewis^Y$-glycosylated peptide antigens leads to enhanced antigen cross-presentation by human Langerhans cells[8,20]. On the other hand, it has been shown that Langerhans cells are not capable of presenting Measles virus (MV) and HIV-1 antigens to cytotoxic $CD8^+$ T cells[14,21]. The glycoproteins decorating the viral envelope of these pathogens are decorated with oligomannosides[22,23]. Internalization and processing of mannosylated antigens via Langerin may therefore deviate from the uptake and processing of Lewis-antigen conjugates. It is known that upon Langerin capture, antigens are endocytosed into Birbeck granules, resulting in antigen degradation. Birbeck granules are rod-like structures that are specific to Langerhans cells and they form a component of the endosomal recycling compartment[24]. It has been shown that Langerin-endocytosed HIV antigens are trafficked to Birbeck granules and rapidly degraded[25]. This clearance of the virus by Langerin-mediated internalization efficiently prevents HIV-1 and measles virus transmission to T cells[14,25]. The mannosylated antigens, under study here, could undergo the same fate, resulting in degradation and minimal antigen presentation and T cell activation as observed here. In contrast, $Lewis^Y$-functionalized peptides are properly loaded onto MHC-I and cross-presented effectively $CD8^+$ T cells[8]. Furthermore, whether only one $Lewis^Y$ moiety was present on the synthetic long peptides, or whether a multivalent $Lewis^Y$-antigen construct was offered to LCs, enhanced cross-presentation was achieved[8,20]. These data suggest the involvement of $Lewis^Y$-mediated routing for successful MHC-I loading and antigen cross-presentation. It thus seems that the nature of the targeting glycan decides the immunological outcome[26].

We have previously described that the mannosylated antigens studied here, can be targeted to APCs expressing DC-SIGN which led to improved antigen uptake. The results obtained with Langerhans cells described here, indicate that in an *in vivo* setting, antigen capture by Langerin can contribute to clearance of the conjugate, thereby necessitating

the use of a higher vaccine dosage to obtain an adequate cytotoxic $CD8^+$ T cell response.

CONCLUSION

In summary, we have described the evaluation of a library of oligomannoside clusters for binding to Langerin. In line with previous results, our study has shown an increase in affinity for the lectin with higher multivalent presentation of the mannoside saccharides. Micromolar binding affinity for the hexavalent compounds was measured, demonstrating their applicability as a Langerin-targeting device. Nonetheless, conjugation of the hexavalent mannoside clusters to the gp100 antigen significantly reduced antigen cross-presentation to $CD8^+$ T cells in two independent $Langerin^+$ APC models, indicating that higher CLR receptor affinity does not have to lead to improved antigen presentation, as we have also observed with DC-SIGN targeting in earlier work[12]. Nevertheless, antigen processing after Langerin-mediated endocytosis and priming of $CD4^+$ T cells could provide a different path to boost the immune response. Further work is required to establish whether antigen presentation to $CD4^+$ T cells is indeed enhanced, as seen with MV[14]. Literature implicates the importance of glycan moiety choice for Langerin targeting, as $Lewis^Y$-functionalized antigens did achieve enhanced Langerin-mediated antigen presentation to cytotoxic T cells[8,20]. The results presented here emphasize the need to validate the glycan moiety in conjugates not only for receptor binding, but also downstream biological effects, such as antigen presentation to $CD8^+$ and $CD4^+$ T cells, effectuated by different cell types, before they can be implemented as immunotherapeutic vaccine.

MATERIALS AND METHODS

General synthesis of the library

The synthesis of the mannoside library has been described in full in earlier work[12].

Cell culture

Langerin expressing Epstein-Barr virus-transformed B-lymphoblastic cells (BLCs) were used as autologous APC[14], and were cultured in RPMI 1640 (Invitrogen) supplemented with 10% FCS (Biowittaker), 1% penicillin and streptomycin (both Lonza). Langerin expressing MUTZ-3-derived LCs were differentiated from the MUTZ-3 progenitor cell line with 100 ng/mL GM-CSF (Biosource), 10 ng/mL TGF-β (R&D Systems), and 2.5 ng/mL TNF-α (Miltenyi)[27].

Surface Plasmon Resonance Analysis

The ECD of Langerin (residues 68-328) was overexpressed and purified as previously

described[24]. The SPR competition experiments were performed on a Biacore T200 using a CM3 series S sensor chip. Control flow cell 1 was functionalized with BSA, while flow cell 2 and 3 were treated with 60 µg/mL BSA-Manα1-3[Manα1-6]Man (Dextra) in 10 mM NaOAc pH 4 (final densities 2.062 and 2.183 RU, respectively). All flow cells were blocked with ethanolamine. The affinities for the Langerin ECD were evaluated via an inhibition assay, using 25 mM tris-HCl pH 8, 150 mM NaCl, 4 mM $CaCl_2$, 0.05% P20 surfactant as running buffer. Langerin ECD (20 µM) was injected at 5 µL/min, with or without inhibitor at increasing concentrations. The data was analyzed in Biacore BIAevaluation software using four parameter equation, and the IC_{50} was determined.

To determine the apparent K_d value, direct interaction experiments were executed on a T200 Biacore with a CM3 series S sensor chip. The Langerin ECD in this assay was functionalized with a StreptagII on the N-terminus (Langerin S-ECD), for oriented capture on the sensor chip surface. The flow cells were functionalized with streptactin protein after EDC/NHS activation. Control flow cell 1 was functionalized with BSA, while another flow cells was functionalized with 100 µg/mL Langerin S-ECD via tag specific capture and simultaneous amine coupling. An approximate density between 2.609 RU was achieved on the chip surface. The compounds were injected in increasing concentrations with a flow rate of 30 µL/min in the previously mentioned running buffer. The data was analyzed in Biacore BIAevaluation software for direct interaction 1:1 calculation to determine the apparent K_d value.

Mannose Library Binding

Approximately 10^5 cells were washed and resuspended in 100 µL pre-cooled (4°C) 1x Hank's Balanced Salt Solution (Gibco), supplemented with 1% BSA. The cells were pre-incubated with 20 µg/mL anti-CD207 (Clone 10E2, in house[25]) in the blocking conditions for 45 minutes on ice. 10 µM of biotin functionalized clusters or 1 µg/mL of biotin functionalized $Lewis^Y$- or mannose-conjugated polyacrylamide as control were added. After 30 minutes incubation on ice, the cells were washed with pre-cooled (4°C) PBS and stained with Alexa647-streptavidin (InvitrogenTM) in PBS supplemented with 0.5% BSA and 0.02% NaN_3. The cells were extensively washed after 30 minutes incubation on ice, and fixed in PBS supplemented with 0.5% PFA. Fluorescence was measured by flow cytometry (CyAnTM APD with SummitTM software), and analyzed using FlowJo v10.

Antigen Presentation

Cells were seeded at $50{\cdot}10^3$ cells/well in a 96-well plate (Greiner) and incubated with 20 µM of the peptide conjugates. The gp100 short peptide ($gp100_{280\text{-}288}$) was taken along as a positive control. After 30 minutes of stimulation, cells were washed and co-cultured with

10^5 $CD8^+$ HLA-A2.1 restricted T cells from a clone transduced with a $gp100_{280-288}$ specific TCR[28]. After overnight stimulation, IFNγ levels in the supernatant were measured by ELISA according to manufacturer's protocol (Biosource), and measured at 450 nm on the iMarkTM Microplate Absorbance Reader (Bio-Rad).

Statistics

The data are presented as the mean ± SD of at least three independent experiments. Statistical analysis was performed in GraphPad Prism v8. Statistical significance was set at $P < 0.05$ and was evaluated by the Mann-Whitney U-test.

CONFLICT OF INTEREST

All authors declare that the research was conducted in the absence of any commercial or financial relationships that could be construed as a potential conflict of interest.

AUTHOR CONTRIBUTIONS

R-JL and TH wrote the first drafts of this manuscript. TH synthesized the described constructs under supervision of DF, GM, and JC. SS cultured and monitored the differentiation of the MUTZ-LCs. R-JL determined the cellular affinity, internalization, and antigen presentation aided by SB under supervision of SV and YK. SA and CV performed the SPR experiments under supervision of FF. MT was involved in the preparation of the SPR samples. All authors revised the manuscript.

FUNDING

This work was funded by the NWO Gravitation programme 2013 granted to the Institute for Chemical Immunology (ICI-024.002.009) and by the European Union's Horizon 2020 research and innovation program under the Marie Sklowdowska-Curie grant agreement No. 642870 (Immunoshape).

The Multistep Protein Purification Platform (MP3) was exploited for human Langerin ECD, and S-ECD production and the SPR platform for the competition and direct interaction tests of the Grenoble Instruct center (ISBG; UMS 3518 CNRS-CEA-UJF-EMBL) with support from FRISBI (ANR-10-INSB-05-02) and GRAL (ANR-10-LABX-49-01) within the Grenoble Partnership for Structural Biology.

ACKNOWLEDGEMENTS

We thank the Sue Gibbs lab for providing the Langerin$^+$ MUTZ cells. We also thank members of the O| 2 Flow Cytometry Facility of Amsterdam UMC – location VUmc for their technical support.

REFERENCES

1 Levin, C.; Perrin, H.; Combadiere, B. Tailored Immunity by Skin Antigen-Presenting Cells. Hum. Vaccin. Immunother. 2015, 11 (1), 27–36. https://doi.org/10.4161/hv.34299.

2 Zaric, M.; Lyubomska, O.; Poux, C.; Hanna, M. L.; McCrudden, M. T.; Malissen, B.; Ingram, R. J.; Power, U. F.; Scott, C. J.; Donnelly, R. F.; et al. Dissolving Microneedle Delivery of Nanoparticle-Encapsulated Antigen Elicits Efficient Cross-Priming and Th1 Immune Responses by Murine Langerhans Cells. J. Invest. Dermatol. 2015, 135 (2), 425–434. https://doi.org/10.1038/jid.2014.415.

3 Stoitzner, P.; Green, L. K.; Jung, J. Y.; Price, K. M.; Tripp, C. H.; Malissen, B.; Kissenpfennig, A.; Hermans, I. F.; Ronchese, F. Tumor Immunotherapy by Epicutaneous Immunization Requires Langerhans Cells. J. Immunol. 2008, 180 (3), 1991–1998. https://doi.org/10.4049/jimmunol.180.3.1991.

4 Santegoets, S. J. A. M.; Bontkes, H. J.; Stam, A. G. M.; Bhoelan, F.; Ruizendaal, J. J.; van den Eertwegh, A. J. M.; Hooijberg, E.; Scheper, R. J.; de Gruijl, T. D. Inducing Antitumor T Cell Immunity: Comparative Functional Analysis of Interstitial versus Langerhans Dendritic Cells in a Human Cell Line Model. J. Immunol. 2008, 180 (7), 4540–4549.

5 Feinberg, H.; Taylor, M. E.; Razi, N.; McBride, R.; Knirel, Y. A.; Graham, S. A.; Drickamer, K.; Weis, W. I. Structural Basis for Langerin Recognition of Diverse Pathogen and Mammalian Glycans through a Single Binding Site. J. Mol. Biol. 2011, 405 (4), 1027–1039. https://doi.org/10.1016/j.jmb.2010.11.039.

6 Wamhoff, E.-C.; Schulze, J.; Bellmann, L.; Rentzsch, M.; Bachem, G.; Fuchsberger, F. F.; Rademacher, J.; Hermann, M.; Del Frari, B.; van Dalen, R.; et al. A Specific, Glycomimetic Langerin Ligand for Human Langerhans Cell Targeting. ACS Cent. Sci. 2019, acscentsci.9b00093. https://doi.org/10.1021/acscentsci.9b00093.

7 Idoyaga, J.; Cheong, C.; Suda, K.; Suda, N.; Kim, J. Y.; Lee, H.; Park, C. G.; Steinman, R. M. Cutting Edge: Langerin/CD207 Receptor on Dendritic Cells Mediates Efficient Antigen Presentation on MHC I and II Products In Vivo. J. Immunol. 2008, 180 (6), 3647–3650. https://doi.org/10.4049/jimmunol.180.6.3647.

8 Fehres, C. M.; Duinkerken, S.; Bruijns, S. C.; Kalay, H.; van Vliet, S. J.; Ambrosini, M.; de Gruijl, T. D.; Unger, W. W.; Garcia-Vallejo, J. J.; van Kooyk, Y. Langerin-Mediated Internalization of a Modified Peptide Routes Antigens to Early Endosomes and Enhances Cross-Presentation by Human Langerhans Cells. Cell. Mol. Immunol. 2017, 14 (4), 360–370. https://doi.org/10.1038/cmi.2015.87.

9 Medve, L.; Achilli, S.; Serna, S.; Zuccotto, F.; Varga, N.; Thépaut, M.; Civera, M.; Vivès, C.; Fieschi, F.; Reichardt, N.; et al. On-Chip Screening of a Glycomimetic Library with C-Type Lectins Reveals Structural Features Responsible for Preferential Binding of Dectin-2 over DC-SIGN/R and Langerin. Chem. - A Eur. J. 2018, 24 (54), 14448–14460. https://doi.org/10.1002/chem.201802577.

10 Varga, N.; Sutkeviciute, I.; Guzzi, C.; McGeagh, J.; Petit-Haertlein, I.; Gugliotta, S.; Weiser, J.; Angulo, J.; Fieschi, F.; Bernardi, A. Selective Targeting of Dendritic Cell-Specific Intercellular Adhesion Molecule-3-Grabbing Nonintegrin (DC-SIGN) with Mannose-Based Glycomimetics: Synthesis and Interaction Studies of Bis(Benzylamide) Derivatives of a Pseudomannobioside. Chem. - A Eur. J. 2013, 19 (15), 4786–4797. https://doi.org/10.1002/chem.201202764.

11 Holla, A.; Skerra, A. Comparative Analysis Reveals Selective Recognition of Glycans by the Dendritic Cell Receptors DC-SIGN and Langerin. Protein Eng. Des. Sel. 2011, 24 (9), 659–669. https://doi.org/10.1093/protein/gzr016.

12 Li, R.-J. E.; Hogervorst, T. P.; Achilli, S.; Bruijns, S. C.; Arnoldus, T.; Vivès, C.; Wong, C. C.; Thépaut, M.; Meeuwenoord, N. J.; van den Elst, H.; et al. Systematic Dual Targeting of Dendritic Cell C-Type Lectin Receptor DC-SIGN and TLR7 Using a Trifunctional Mannosylated Antigen. Front. Chem. 2019, 7, 650. https://doi.org/10.3389/fchem.2019.00650.

13 Feinberg, H.; Powlesland, A. S.; Taylor, M. E.; Weis, W. I. Trimeric Structure of Langerin. J. Biol. Chem. 2010, 285 (17), 13285–13293. https://doi.org/10.1074/jbc.M109.086058.

14 van der Vlist, M.; de Witte, L.; de Vries, R. D.; Litjens, M.; de Jong, M. A. W. P.; Fluitsma, D.; de Swart, R. L.; Geijtenbeek, T. B. H. Human Langerhans Cells Capture Measles Virus through Langerin and Present Viral Antigens to CD4+ T Cells but Are Incapable of Cross-Presentation. Eur. J. Immunol. 2011, 41 (9), 2619–2631. https://doi.org/10.1002/eji.201041305.

15 Fehres, C. M.; Kalay, H.; Bruijns, S. C. M.; Musaafir, S. A. M.; Ambrosini, M.; Bloois, L. van; van Vliet, S. J.; Storm, G.; Garcia-Vallejo, J. J.; Van Kooyk, Y. Cross-Presentation through Langerin and DC-SIGN Targeting Requires Different Formulations of Glycan-Modified Antigens. J. Control. Release 2015, 203, 67–76. https://doi.org/10.1016/j.jconrel.2015.01.040.

16 Banchereau, J.; Thompson-Snipes, L.; Zurawski, S.; Blanck, J.-P.; Cao, Y.; Clayton, S.; Gorvel, J.-P.; Zurawski, G.; Klechevsky, E. The Differential Production of Cytokines by Human Langerhans Cells and Dermal CD14+ DCs Controls CTL Priming. Blood 2012, 119 (24), 5742–5749. https://doi.org/10.1182/blood-2011-08-371245.

17 Polak, M. E.; Thirdborough, S. M.; Ung, C. Y.; Elliott, T.; Healy, E.; Freeman, T. C.; Ardern-Jones, M. R. Distinct Molecular Signature of Human Skin Langerhans Cells Denotes Critical Differences in Cutaneous Dendritic Cell Immune

Regulation. J. Invest. Dermatol. 2014, 134 (3), 695–703. https://doi.org/10.1038/JID.2013.375.

18 de Jong, M. A. W. P.; de Witte, L.; Santegoets, S. J. A. M.; Fluitsma, D.; Taylor, M. E.; de Gruijl, T. D.; Geijtenbeek, T. B. H. Mutz-3-Derived Langerhans Cells Are a Model to Study HIV-1 Transmission and Potential Inhibitors. J. Leukoc. Biol. 2010, 87 (4), 637–643. https://doi.org/10.1189/jlb.0809577.

19 Czubala, M. A.; Finsterbusch, K.; Ivory, M. O.; Mitchell, J. P.; Ahmed, Z.; Shimauchi, T.; Karoo, R. O. S.; Coulman, S. A.; Gateley, C.; Birchall, J. C.; et al. TGFβ Induces a SAMHD1-Independent Post-Entry Restriction to HIV-1 Infection of Human Epithelial Langerhans Cells. J. Invest. Dermatol. 2016, 136 (10), 1981–1989. https://doi.org/10.1016/J.JID.2016.05.123.

20 Duinkerken, S.; Horrevorts, S. K.; Kalay, H.; Ambrosini, M.; Rutte, L.; de Gruijl, T. D.; Garcia-Vallejo, J. J.; van Kooyk, Y. Glyco-Dendrimers as Intradermal Anti-Tumor Vaccine Targeting Multiple Skin DC Subsets. Theranostics 2019, 9 (20), 5797–5809. https://doi.org/10.7150/thno.35059.

21 van den Berg, L. M.; Cardinaud, S.; van der Aar, A. M. G.; Sprokholt, J. K.; de Jong, M. A. W. P.; Zijlstra-Willems, E. M.; Moris, A.; Geijtenbeek, T. B. H. Langerhans Cell-Dendritic Cell Cross-Talk via Langerin and Hyaluronic Acid Mediates Antigen Transfer and Cross-Presentation of HIV-1. J. Immunol. 2015, 195 (4), 1763–1773. https://doi.org/10.4049/jimmunol.1402356.

22 Hashiguchi, T.; Kajikawa, M.; Maita, N.; Takeda, M.; Kuroki, K.; Sasaki, K.; Kohda, D.; Yanagi, Y.; Maenaka, K. Crystal Structure of Measles Virus Hemagglutinin Provides Insight into Effective Vaccines. Proc. Natl. Acad. Sci. U. S. A. 2007, 104 (49), 19535–19540. https://doi.org/10.1073/pnas.0707830104.

23 Bonomelli, C.; Doores, K. J.; Dunlop, D. C.; Thaney, V.; Dwek, R. A.; Burton, D. R.; Crispin, M.; Scanlan, C. N. The Glycan Shield of HIV Is Predominantly Oligomannose Independently of Production System or Viral Clade. PLoS One 2011, 6 (8), e23521. https://doi.org/10.1371/journal.pone.0023521.

24 Thépaut, M.; Valladeau, J.; Nurisso, A.; Kahn, R.; Arnou, B.; Vivès, C.; Saeland, S.; Ebel, C.; Monnier, C.; Dezutter-Dambuyant, C.; et al. Structural Studies of Langerin and Birbeck Granule: A Macromolecular Organization Model † ‡. Biochemistry 2009, 48 (12), 2684–2698. https://doi.org/10.1021/bi802151w.

25 de Witte, L.; Nabatov, A.; Pion, M.; Fluitsma, D.; de Jong, M. A. W. P.; de Gruijl, T.; Piguet, V.; van Kooyk, Y.; Geijtenbeek, T. B. H. Langerin Is a Natural Barrier to HIV-1 Transmission by Langerhans Cells. Nat. Med. 2007, 13 (3), 367–371. https://doi.org/10.1038/nm1541.

26 Geijtenbeek, T. B. H.; Gringhuis, S. I. C-Type Lectin Receptors in the Control of T Helper Cell Differentiation. Nat. Rev. Immunol. 2016, 16 (7), 433–448. https://doi.org/10.1038/nri.2016.55.

27 de Jong, M. A. W. P.; de Witte, L.; Santegoets, S. J. A. M.; Fluitsma, D.; Taylor, M. E.; de Gruijl, T. D.; Geijtenbeek, T. B. H. Mutz-3-Derived Langerhans Cells Are a Model to Study HIV-1 Transmission and Potential Inhibitors. J. Leukoc. Biol. 2010, 87 (4), 637–643. https://doi.org/10.1189/jlb.0809577.

28 Schaft, N.; Willemsen, R. A.; de Vries, J.; Lankiewicz, B.; Essers, B. W. L.; Gratama, J.-W.; Figdor, C. G.; Bolhuis, R. L. H.; Debets, R.; Adema, G. J. Peptide Fine Specificity of Anti-Glycoprotein 100 CTL Is Preserved Following Transfer of Engineered TCRαβ Genes Into Primary Human T Lymphocytes. J. Immunol. 2003, 170 (4), 2186–2194. https://doi.org/10.4049/jimmunol.170.4.2186.

SUPPLEMENTARY

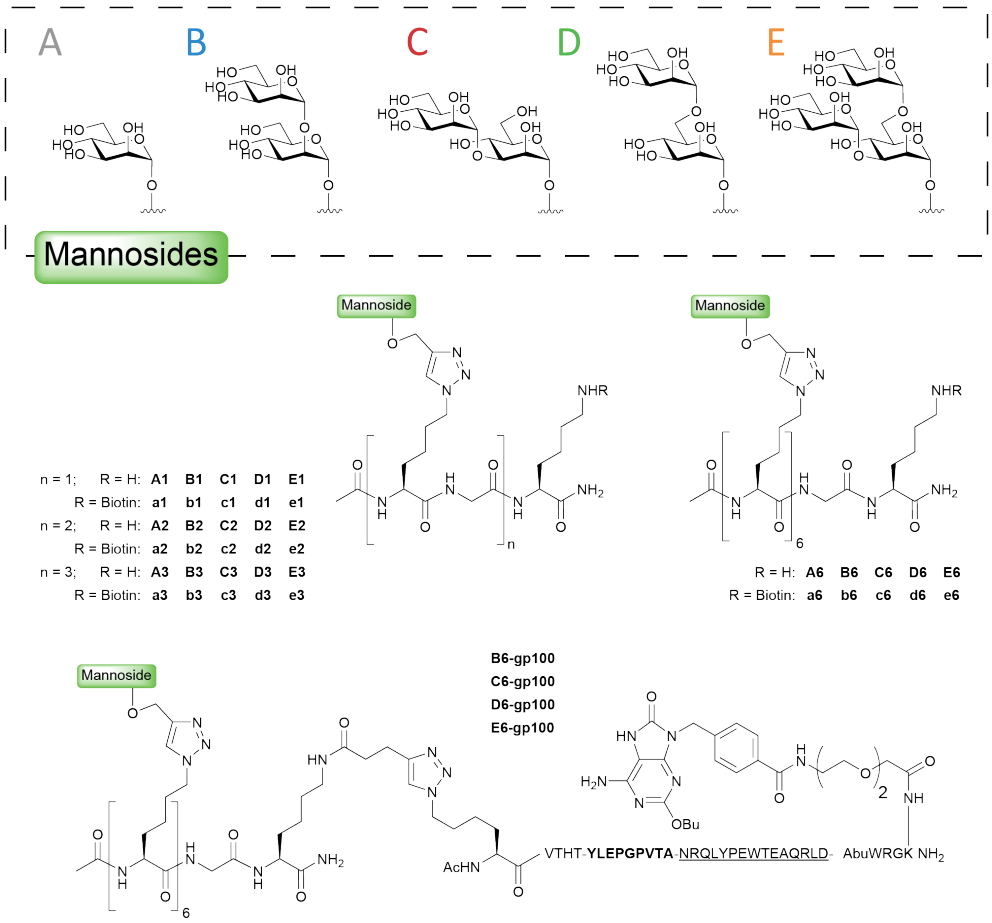

SI.Figure 1 | Schematic overview of the mannosylated compounds Five mannosides (upper panel) with 1, 2, 3, or 6 copy numbers were used to synthesize the library of 20 constructs (middle panel). The alkyne handle could also be functionalized with a biotin, resulting in a biotynilated cluster (coded with a lower case). In the lower panel, the clusters were functionalized with a gp100$_{280\text{-}288+44\text{-}59}$ antigen.

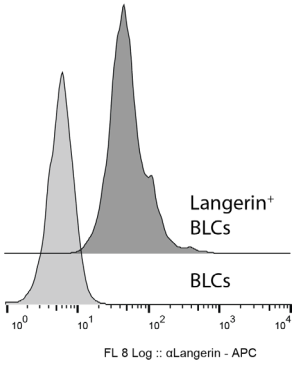

SI.Figure 2 | Langerin expression of Langerin$^+$ BLCs. Flowcytometric quantification of Langerin expression of the the BLCs and Langerin transfected BLCs demonstrate only expression in the Langerin$^+$ BLCs.